Published in final edited form as:

*Arterioscler Thromb Vasc Biol*. 2016 April ; 36(4): 718–727. doi:10.1161/ATVBAHA.115.306748.

# Glycosphingolipids on human myeloid cells stabilize E-selectin dependent rolling in the multistep leukocyte adhesion cascade

**Nandini Mondal**[1], **Gino Stolfa**[1], **Aristotelis Antonopoulos**[4], **Yuqi Zhu**[1], **Shuen-Shiuan Wang**[1], **Alexander Buffone Jr.**[1], **G. Ekin Atilla-Gokcumen**[2], **Stuart M. Haslam**[4], **Anne Dell**[4], and **Sriram Neelamegham**[1,3]

[1]Department of Chemical and Biological Engineering, State University of New York, Buffalo, NY 14260, USA

[2]Department of Chemistry, State University of New York, Buffalo, NY 14260, USA

[3]The NY State Center for Excellence in Bioinformatics and Life Sciences, State University of New York, Buffalo, NY 14260, USA

[4]Department of Life Sciences, Imperial College London, London, SW7 2AZ, UK

## Abstract

**Objective—**Recent studies suggest that the E-selectin ligands expressed on human leukocytes may differ from those in other species, particularly mice. To elaborate on this, we evaluated the impact of glycosphingolipids (GSLs) expressed on human myeloid cells in regulating E-selectin mediated cell adhesion.

**Approach and Results—**A series of modified human cell lines and primary neutrophils were created by targeting UDP-Glucose Ceramide Glucosyltransferase (UGCG) using either lentivirus delivered shRNA or CRISPR-Cas9 based genome editing. Enzymology and mass spectrometry confirm that the modified cells had reduced or abolished glucosylceramide biosynthesis. Glycomics profiling showed that UGCG disruption also increased prevalence of bisecting N-glycans and reduced overall sialoglycan expression on leukocyte N- and O-glycans. Microfluidics based flow chamber studies demonstrated that both the UGCG knockouts and knockdowns display ~60% reduction in leukocyte rolling and firm adhesion on E-selectin bearing stimulated endothelial cells (ECs), without altering cell adhesion to P-selectin. Consistent with the concept that the GSLs support slow rolling and the transition to firm arrest, inhibiting UGCG activity resulted in frequent leukocyte detachment events, skipping motion and reduced diapedesis across the endothelium. Cells bearing truncated O- and N-glycans also sustained cell rolling on E-selectin, although their ability to be recruited from free fluid flow was diminished.

**Conclusions—**GSLs likely contribute to human myeloid cell adhesion to E-selectin under fluid shear, particularly the transition of rolling cells to firm arrest.

Correspondence: Prof. Sriram Neelamegham, 906 Furnas Hall, State University of New York, Buffalo, NY 14260, USA; Tel.: (716) 645-1200; Fax: (716) 645-3822; neel@buffalo.edu.

Disclosures: The authors declare no conflict of interest.

**Keywords**

cell adhesion molecule; flow shear stress; leukocyte; endothelial cell; inflammation

## INTRODUCTION

P- (CD62P), E- (CD62E) and L-selectin (CD62L) constitute a family of C-type lectins that initiate the multi-step process of leukocyte recruitment at sites of inflammation[1-3]. Among these, P- and E-selectin are expressed on stimulated endothelial cells and they mediate the direct capture of leukocytes to the inflamed vessel. L-selectin is expressed on leukocytes and this facilitates secondary capture via leukocyte-leukocyte adhesion. All members of the selectin family bind cell-surface glycoconjugates expressed on blood leukocytes with rapid on- and off-rates in a calcium dependent manner[4-6]. Such high on-rates enable the capture or tethering of leukocytes from flowing blood. Following this, a succession of rapid bond formation and breakage events results in cell rolling on the vessel wall. Rolling provides residence time during which leukocytes can be activated by chemokines expressed on the inflamed endothelium and also via signaling through selectin-ligand bonds. This then leads to firm adhesion and leukocyte diapedesis across the vascular endothelium. Similar to leukocyte adhesion during inflammation, selectin mediated binding also regulates lymphocyte homing, hematopoietic stem cell migration and cancer metastasis.

Our knowledge regarding the glycoconjugates that bind selectins during inflammation comes, in large part, from studies using transgenic mice or human blood. Such studies have demonstrated that the sialyl Lewis-X ($sLe^X$) tetrasaccharide attached to a core-2 O-glycan at the N-terminus of P-selectin glycoprotein ligand-1 (PSGL-1, CD162) is a major ligand for P- and L-selectin in both humans and mice[7-9]. Whereas only 2% of the overall O-glycans of human PSGL-1 contain the $sLe^X$ core-2 O-glycan[10], in myeloid cells, this structure constitutes ~20% of the carbohydrates at Thr-57 on the N-terminus of this glycoprotein[11]. With regard to E-selectin, the physiological carbohydrate ligands likely differ between mice and humans[1, 3]. Notably, the rolling of mouse neutrophils on E-selectin is protease sensitive but this is not the case for human leukocytes[12, 13]. Further, while the E-selectin ligands in mouse neutrophils have largely been identified to include PSGL-1, E-selectin Ligand-1 (ESL-1) and CD44[14], the major players in humans remain unknown[1, 3]. In this regard, PSGL-1 is a relatively minor ligand for human E-selectin and there is no homolog for ESL-1 in humans[1, 15]. Also, functional sialofucosylated CD44 glycoforms do not exist in mature leukocytes[16]. Other candidate E-selectin glycoconjugate ligands in humans include CD43, integrin Mac-1, L-selectin and glycosphingolipids (GSLs)[1-3]. The absolute and relative importance of these macromolecules to human leukocyte adhesion remains unknown.

Among the E-selectin ligands, the current study evaluated the potential importance of GSLs during selectin-dependent myeloid cell adhesion since proof supporting their functional importance is incomplete. In this regard, previous studies have suggested that a group of sialofucosylated lactosylceramides called ‘myeloglycans’ can bind E-selectin[17, 18]. These GSLs contain 4 or more N-acetyllactosamine (LacNAc) repeats, with one or more internal fucose

residues[18].NeuAcα2,3Galβ1,4GlcNAcβ1,3[Galβ1,4(Fucα1,3)GlcNAcβ1,3]$_2$[Galβ1,4GlcNAcβ1,3]$_2$Galβ1,4GlcβCer represents a prototypic myeloglycan selectin-ligand[19, 20]. In these studies, myeloglycans extracted from HL-60s[19] and also primary human neutrophils[20] were shown to support the rolling of CHO-E (E-selectin expressing Chinese Hamster Ovary) cells under shear. Additionally, inhibition of glycolipid biosynthesis by the small molecule P4 (D-threo-1-phenyl-2-palmitoylamino-3-pyrrolidino-1-propanol) for 24h partially (~50%) reduced neutrophil binding to immobilized E-, but not P-, selectin under static conditions[20]. However, these studies were not conducted under fluid shear, a necessary condition to demonstrate the physiological relevance of the GSL ligands[21]. Further, pharmacological treatments can have non-specific effects and the short-term (24h) treatment may leave residual GSLs on cells that did not turnover rapidly.

In the current study, we developed shRNA based knockdown and CRISPR-Cas9 based knockout strategies to disrupt lactosylceramide biosynthesis since this provides a specific strategy to evaluate the ability of the GSLs to function as E-selectin ligands. To this end, we targeted UDP-Glucose Ceramide Glucosyltransferase (UGCG)[20, 22, 23] since mammalian hematopoietic cells primarily contain glucosylceramides with a neo-lacto core (Galβ1–4GlcNAcβ1–3Galβ1–4Glcβ1-Cer)[24]. This strategy was applied to HL-60 promyelocytic leukocytes, HL-60s differentiated to neutrophils, and primary neutrophils derived from human hematopoietic stem cells (hHSCs). The results show that UGCG disruption both prevents stable human granulocyte rolling and reduces diapedesis across inflamed endothelial cells. Thus, GSL binding to endothelial E-selectin may control the transition from myeloid cell rolling to firm arrest at sites of inflammation.

## MATERIALS AND METHODS

Materials and Methods are available in the online-only Data Supplement.

## RESULTS

### Human but not mouse leukocyte adhesion to E-selectin is pronase insensitive

We sought to confirm that human leukocyte and HL-60 rolling on E-selectin is pronase (a mixture of proteases) insensitive[12, 13] (Figure 1). Here, mouse neutrophil rolling and adhesion on E-selectin (stimulated HUVECs) was abrogated by pronase (Figure 1A). This was not the case for either primary human neutrophils (Fig. 1B) or HL-60 cells (Fig. 1C). In both Fig. 1B-C, pronase decreased the number of adherent cells without altering cell rolling density. On recombinant P-selectin, the rolling of all cell types was abolished by pronase (Fig. 1D-F). Blocking mAbs against human (KPL1) and mouse (2PH1) PSGL-1, abrogated rolling on P- (bottom row) but not E-selectin. Thus, the N-terminus of PSGL-1 does not contain a major E-selectin ligand (top row).Additional controls confirmed that the molecular interactions in Fig. 1A-C could be completely blocked by anti-E-selectin mAbs (HAE-1f or P2H3) and cell binding in Fig. 1D-F was abrogated by anti-P-selectin mAb G1 (data not shown,[7, 25, 26]).

To evaluate the effectiveness of pronase on reducing cell surface glycoprotein levels, the binding of a panel of mAbs to human neutrophils and HL-60s was evaluated (Supplemental

Table I). Here, the binding of some of mAbs like anti-PSGL-1 was dramatically reduced by pronase, whereas others like anti-CD45 and mAb HECA-452 were only partially (~60%) reduced. Cell surface Mac-1/CD11b was reduced by 62-87%, and this may account for the reduced firm adhesion noted in Fig. 1B-C. Overall, differences between mouse and human leukocyte rolling on E-selectin were confirmed. This effect could be due to GSL ligands on human cells, and/or residual glycoprotein E-selectin ligands that were not digested by pronase, and/or the exposure of new functional epitopes in humans that were previously cryptic.

## Silencing UGCG in HL-60s

ShRNA was applied to silence UGCG on HL-60s in order to address the shortcomings of the pronase approach (Figure 2). This caused a 93% reduction in UGCG mRNA expression as measured by quantitative RT-PCR (Supplemental Table II, III). Stable UGCG knockdown HL60s (i.e. UGCG$^{-}$HL-60) with red fluorescence were then obtained by inserting a DsRed reporter in the lentiviral vector (Fig. 2A). Reduction in UGCG enzyme activity in these DsRed positive UGCG$^{-}$HL-60s was confirmed by enzymology (Fig. 2B). Here, the C6-NBD-Cer substrate was converted to C6-NBD-GlcCer upon addition of UDP-Glc and WT HL-60 cell lysates (lane 1). The TLC $R_f$ values of 0.6 and 0.79 for C6-NBD-GlcCer and C6-NBD-Cer matched previous reports[27]. In the UGCG$^{-}$HL-60s, UGCG enzymatic activity was reduced by ~80% (lane 2). No product was observed when either the cell lysate was absent (lane 5) or when GDP-Fuc replaced UDP-Glc (lane 6). Using flow cytometry (Fig. 2C), the UGCG$^{-}$HL-60s displayed a ~75% reduction in sLe$^{X}$ and related epitopes recognized by mAb HECA-452 (left panel) and ~35% reduction in mAb CSLEX-1 binding (middle).

UGCG$^{-}$HL-60 rolling on P-selectin under fluid shear was identical to WT HL-60s (Supplemental Fig I). Thus, the core-2 sLe$^{X}$ at the N-terminus of PSGL-1 remained intact in the knockdown cells. In contrast, UGCG silencing reduced HL-60 rolling density on E-selectin bearing stimulated HUVECs by ~60% (Fig. 2D), and augmented cell rolling velocity by 2-fold (Fig. 2E).Anti-PSGL-1 mAb KPL-1 abolished UGCG$^{-}$HL-60 rolling on P-selectin but not HUVECs. Pronase reduced the number of adherent UGCG$^{-}$HL-60s on HUVECs without affecting cell rolling density. The residual rolling could be either due to incomplete UGCG silencing or pronase insensitive selectin-ligands. Overall, disrupting GSL biosynthesis reduced cell rolling on E-selectin.

## Genome editing and glycome analysis of UGCG-KOs

Genome editing allows complete deletion of specific enzyme activity unlike RNAi, which is incomplete [25, 28]. HL-60 knockouts were thus generated using CRISPR-Cas9 method (Figure 3). The UGCG-KO cell line thus created contained a 16bp chromosomal deletion as seen in the sequencing results (Fig. 3A). Only one UGCG allele was sequenced here since UGCG is present on chromosome-9, and spectral karyotyping of HL-60 demonstrates the loss of the second copy due to a chromosome-9 translocation [29]. The absence of off-target editing was also confirmed by sequencing all potentially similar exonic off-target sites. Consistent with this, enzymology based TLC demonstrates the complete loss of UGCG activity in the UGCG-KO cell lysates (Supplemental Fig. II). Loss of glycolipids was also confirmed using LC-MS based lipidomics analysis (Supplemental Fig. III, [30, 31]). Here,

C16- , C24-HexCer and C16-, C24-$(Hex)_2$Cer were detected in WT HL-60s, but these were completely depleted in the UGCG-KOs.

UGCG-KO HL-60s displayed ~80% reduction in CLA/HECA-452 (Fig. 3B: Top left), ~50% reduction in $sLe^X$ expression (Top right) and a small decrease in $Le^X$ expression (Bottom left). These findings are very similar to the UGCG$^-$HL-60 results (Fig. 2C). MAb VIM-2 expression was unchanged suggesting that this reagent may also recognize glycans on non-GSL glycoconjugates (Fig. 3B: Bottom right,[32]). In lectin binding studies, the UGCG-KOs did not show substantial changes in N-glycan structures as measured using L-PHA (*Phaseolus vulgaris Leucoagglutinin*) binding, or overall sialylation using both Mal-II (*Maackia Amurensis* lectin-II) and PNA lectin (*Peanut lectin*) (Fig. 3C).

The decrease in the HECA-452 epitope upon knocking-out/down UGCG prompted detailed mass spectrometric profiling of HL-60 associated N- (Fig. 3D, Supplemental Fig. IV-VI) and O-glycans (Fig. 3E). Here, MALDI-TOF MS revealed a complex N-glycan profile in WT HL60s consisting of multi-antennary structures decorated with varying levels of fucose and sialic acid (NeuAc) similar to previous work [25] (Fig. 3D upper panel and Supplemental Fig. IV). Disrupting UGCG resulted in less sialylated structures and a concomitant increase in bisected N-glycans (Fig. 3D lower panel, Supplemental Fig. IV).The knockdown UGCG$^-$HL-60s also displayed an intermediate relative abundance of the sialylated and bisected N-glycans (Supplemental Fig. V). MALDI-TOF MS and MALDI-TOF/TOF MS/MS (Supplemental Fig. VI) analysis of N-glycans subjected to endo-β-galactosidase digestion revealed the extent of polylactosamine repeats (poly-LacNAcs) and defined the terminal epitopes on extended antennae. Here, compared to undecorated LacNAc (*m/z* 722), we noted a partial decrease in sialylated LacNAc (*m/z* 1083, 55%), $sLe^X$ (*m/z* 1257, 33%) and VIM-2 (*m/z* 1706, 15%) upon knocking-out UGCG (Fig. S6, left vs. right panels, Supplemental Table IV). Poly-LacNAcs (*m/z* 518) and $Le^X$ terminal epitopes (*m/z* 896 and 1519) remained unaltered. No major difference was detected in the relative abundance of multi-branched N-glycans except for a ~30% decrease in tetra-antennary N-glycans in the UGCG-KO HL-60s (Supplemental Table V).

The O-glycan profile of the WT HL-60s consisted of core-1 (*m/z* 895 and 1256) and core-2 (*m/z* 983, 1344, 1518 and 1879) structures (Fig. 3E, top panel) [25]. In the UGCG-KO HL-60s, overall, similar structures were observed, however accompanied by a decreased sialylation (Fig. 3F, bottom panel).In this regard, we noted a decrease in the double sialylated-Tn antigen (*m/z* 1256) over the sialylated-Tn antigen (*m/z* 895), a decrease of the double sialylated core 2 O-glycan (*m/z* 1705) over the monosialylated core 2 O-glycan (*m/z* 1344) and a reduction in core-2 O-glycans carrying the $sLe^X$ terminal epitope (*m/z* 1879) (Fig.3D, top vs. bottom panels). Thus, a decrease in N- and O-glycan sialylation accompanied UGCG silencing/deletion.

## UGCG-KO HL-60s exhibit skipping motion on stimulated endothelial cells

The effect of UGCG disruption on cell rolling and adhesion was quantified (Figure 4, Movie A). Here, consistent with the silencing approach, the UGCG-KO HL60s displayed a 50% reduction in cell rolling and 70% reduction in firm adhesion density on stimulated HUVECs where cell adhesion is E-selectin dependent (Fig. 4A). Pronase did not alter the total number

of interacting cells, though it decreased the proportion of adherent cells and increased the median rolling velocity of both the WT and UGCG-KO HL-60s by ~1.5-2-fold (Fig. 4B). UGCG-KOs treated with pronase exhibited a 3-4 fold higher median rolling velocity compared to the WT HL-60s. Similar partial reduction in cell rolling density and 3-fold increased in cell rolling velocity was observed when the knockouts cells were perfused over recombinant E-selectin substrates (Supplemental Fig VII).

Detailed 'tethering analysis' on stimulated HUVECs confirmed that the disruption of GSL biosynthesis may reduce the stability of leukocyte rolling (Fig. 4C-F). Here, the number of tethers formed was similar for all treatments (Fig. 4C). Among these cells, only 5% cell detachment was observed in the case of WT HL-60s with 65% of the tethered cells eventually transitioning to firm arrest over 4 min (Fig. 4D). For all other treatments the number of adherent cells decreased dramatically. Both pronase treatment and knocking out UGCG caused 50-60% of the tethered cells to detach in the experimental window. Detachment was even higher (~80%) when pronase was applied to the UGCG-KO HL-60s.The additive effect of pronase and UGCG-deletion was also noted upon following individual cell trajectories (Fig. 4E, F). Here, the WT HL-60s exhibited robust rolling with low, stable velocities (top panels). Pronase (second panel) and UGCG gene disruption (third from top) often increased instantaneous rolling velocities to 200-250μm/s, with frequent cell skipping motion leading to detachment events. Thus, the cumulative distance travelled by these cells was higher. The strength of cell interactions was further decreased upon pronase treatment of UGCG-KO HL60s (Fig. 4F). Similar experimental results as with the UGCG-KOs were also observed upon performing tethering analysis on the UGCG$^{-}$HL-60s (Supplemental Fig VIII).

## UGCG disruption reduced cell transmigration

HL-60s were differentiated towards neutrophils using DMSO in order to determine if reduced UGCG activity affects leukocyte transmigration across HUVEC monolayers (Figure 5, Movie B). During such differentiation, HL-60 cell size decreased to more closely resemble the size of primary human neutrophils. CD11b expression on the WT HL-60s also increased 5-fold over 5-days, with cell differentiation proceeding markedly faster for the UGCG-KOs and UGCG$^{-}$HL-60s (Fig. 5A). While the sLe$^{X}$ expression on the undifferentiated UGCG-KO was low compared to WT-HL-60s, the HECA-452 binding/sLe$^{X}$ expression was comparable for both cells upon differentiation. Further, Le$^{X}$ levels were reduced for all cell types at day-5. Upon differentiation, the WT, UGCG$^{-}$HL-60s and UGCG-KOs all acquired an ability to transmigrate across the endothelium.

Both the undifferentiated and differentiated HL-60s displayed rolling and firm adhesion interactions though the fraction of cells transitioning to firm arrest was higher for the differentiated cells. This is presumably due to the smaller size and higher Mac-1 expression levels of the differentiated cells (Fig. 1C vs. Fig. 5B). A ~50-60% reduction in rolling and adherent cell density was observed for both the differentiated UGCG$^{-}$ and UGCG-KO HL-60s compared to WT. Whereas pronase only partially reduced the number of adherent cells in the case of differentiated WT HL60s, it reduced the total number of interacting cells

by ~80-90% in the case of the differentiated cells lacking UGCG (both knockdowns and knockouts).

In static transmigration assays, differentiated HL-60 transmigration was reduced by anti-CD18 blocking mAb IB4 consistent with previous data[33] and it was abolished by pronase (Fig. 5D). The anti-E-selectin mAb P2H3 partially reduced transmigration efficacy although the effect did not reach statistical significance. In addition, both the UGCG knock-downs and knock-outs displayed reduced transmigration by 50-60% under static conditions. The effect of UGCG disruption on leukocyte transmigration was more prominent under hydrodynamic shear (65-80% reduction), likely due to the reduced recruitment of these cells on E-selectin expressing stimulated HUVECs under flow (Fig. 5C).

### UGCG disruption reduces the recruitment of primary neutrophils derived from hHSCs

To determine the role of the GSLs in regulating primary human myeloid cell adhesion, lentiviral gene silencing was performed on CD34+ hHSCs while they were being differentiated towards neutrophils (Figure 6).This typically resulted in ~25-35% red-fluorescence cells since both the control and UGCG shRNA virus carried a DsRed reporter (Fig. 6A). Microfluidics-based cell adhesion assays then followed the transduced, fluorescent control (‘DsRed-Neu’) and knockdown (‘UGCG$^{-}$-Neu’) cells. Here, on IL-1β stimulated HUVEC monolayers, a ~50% reduction of cell adhesion was robustly observed in hHSC derived UGCG$^{-}$ neutrophils compared to the DsRed$^{+}$ controls (Fig. 6B). Thus, similar to the HL-60s, attenuation of UGCG activity reduced primary granulocyte adhesion under physiological flow.

## DISCUSSION

Methods to disrupt E-selectin mediated cell adhesion and the identification of physiological human E-selectin ligands is important, both in the context of inflammatory diseases and hematopoietic stem cell homing [1, 3]. This is because leukocyte rolling on E-selectin results in slower rolling velocities compared to L- and P-selectin, due to low molecular binding on- and off-rates [26, 34, 35]. Such slow rolling enhances leukocyte-endothelium contact, facilitating enhanced cell activation, the conversion of rolling cells to firm arrest and diapedesis. Additionally, unlike the human ortholog, the murine *Selp* gene is uniquely responsive to inflammatory cytokines like TNF-α and IL-1β as it has binding sites for multiple transcription factors including NF-κB and ATF-2 [36]. Since our understanding regarding the relevance of selectins largely comes from murine disease models where P-selectin has an exaggerated role, it is possible that current literature underestimates the contributions of E-selectin to human ailments. Finally, the physiological E-selectin ligands in humans are unknown and their definition is clinically significant as it can identify new anti-inflammatory drug targets.

This work suggests that the GSLs are likely to be critical E-selectin ligands specific to human leukocytes. Under the most stringent conditions, the demonstration that a particular molecule is a functional selectin-ligand requires that it satisfy four criteria (modified from [21]). First, the ligand should be expressed in the right place at the right time. This is

satisfied by the GSLs as they are expressed on the human myeloid cell surface, and they bear various sialofucosylated glycans [18, 20, 25].

Second, it should recognize selectins with high affinity, as demonstrated previously for E-selectin-GSL interactions [18-20]. These investigators extracted a group of relatively low abundance, sialofucosylated GSLs collectively termed ‘myeloglycans’ from both primary human neutrophils and HL-60s. These monosialogangliosides contained extended 5-6 lactosamine repeat units, terminal α2,3-sialylation and multiple internal fucose residues. When reconstituted as a substrate in parallel-plate flow chambers, the myeloglycans supported the rolling of E-selectin expressing CHO-E cells under flow.

Third, the deletion of these molecules in relevant cell types should alter selectin mediated cell adhesion. In this regard, while previous studies used small molecule inhibitors to reduce leukocyte GSL content [20], adhesion assays under fluid shear could not be performed after pharmacological treatment since human peripheral blood neutrophils are short-lived and the cells adopted an irregular shape when cultured. This limitation is addressed here using precise gene silencing and genome editing to reduce UGCG activity in human myeloid cells. While the UGCG mRNA levels and enzyme activity were reduced by 93% and 80% respectively in the knockdowns, enzyme activity was abolished in the knockouts. Very similar changes in cell surface glycan expression and rolling was observed using both the knockouts and knockdowns, suggesting that the findings reported here are robust. Similar observations were also made with different cell types including wild-type HL60s, differentiated HL-60s and primary neutrophils derived from hHSCs.

With respect to the detailed functional role of the GSLs, UGCG disruption did not affect the leukocyte tethering rates on E-selectin bearing stimulated HUVECs under flow. However, while wild-type HL-60s displayed continuous slow rolling, both the knock-outs and knock-downs displayed skipping motion that was characterized by high intermittent instantaneous velocities. Here, leukocytes released from the stimulated HUVEC monolayer were recaptured downstream in a fraction of the cases. The unstable motion of the UGCG deficient cells resulted in ~50-60% reduction in the number of rolling and adherent cells on the HUVEC monolayer. Median rolling velocity was also increased by 2-fold. These data are consistent with the notion that the GSLs promote slow rolling on the endothelium since they reside closer to the cell membrane compared to the glycoproteins which extend further away. Such slow rolling may promote the transition of tethered and rolling cells to firm arrest.

The fourth and most stringent requirement to demonstrate that a given molecule is a functional selectin ligand is that function blocking mAbs or other specific reagents that can perturb one molecular interaction without altering other bystanders must be developed. To date, the only selectin-ligand to fully satisfy this criterion is PSGL-1 for which function blocking mAbs are available [37].To determine if similar specificity can be established for the UGCG-knockout/down approach, we performed both flow cytometry with functionally relevant mAbs/lectins and comprehensive glycomic profiling of N-/O-glycans. Here, the glycans in the WT and KO cells were qualitatively identical, albeit with some quantitative differences. First, while PHA-L lectin binding did not show a change in the pattern of N-

glycan branching, glycomics profiling revealed an increased prevalence of bisected N-glycans. Based on quantitative RT-PCR, this change can be explained by a decrease in the mRNA levels of the branching GlcNActransferases (GnT-IV and -V) upon UGCG disruption which may account for the apparent increase in activity of the bisecting enzyme, GnT-III (Supplemental Fig. IX).Second, knocking out UGCG reduced the binding of two mAbs that bind $sLe^X$ and related epitopes on O-glycans, N-glycans and GSLs, HECA-452[38-40] (70% reduction) and CSLEX-1[41] (35% reduction). A reduction in N- and O-linked sialoglycan expression was also noted using glycomics profiling. Thus, alterations in the glycolipid pathway have 'systems-level' effects that perturb the output of other apparently unrelated pathways. Additional studies are necessary to more precisely define the regulation of these glycosylation gene regulatory networks [42]. This may explain why the perturbation of glycolipid biosynthesis results in a more profound reduction in transendothelial migration compared to the blockade of E-selectin binding function.

To more precisely determine if the reduced cell adhesion properties of the UGCG deficient cells are directly due to the contribution of the GSLs to leukocyte adhesion or if they are an indirect effect due to changes in O-/N-glycans, we created additional CRISPR-Cas9 HL-60-KO variants where the biosynthesis of O- and N-glycans was abrogated by knocking out the T-synthase chaperone *COSMC* and GlcNAcT-I gene *MGAT1* (G.S. *et al.*, in preparation). These dual knockouts lacking O- and N-glycans displayed reduced cell surface $sLe^X$ expression. While these cells were not recruited onto E-selectin substrates efficiently under continuous fluid shear, they could sustain cell rolling if captured under static conditions prior to a ramped increase in applied shear. Taken together with the UGCG-KO data presented in the current manuscript, these observations support a role for the GSLs in sustaining the slow rolling of human myeloid cells. Due to this, the abrogation of GSL biosynthesis reduced the transition of the rolling cells to firm arrest and subsequent extravasation.

In conclusion, human genetic perturbation studies in the current manuscript show that the GSLs are likely to function as E-selectin ligands that facilitate the transition of rolling human myeloid cells to firm arrest. It would be interesting to determine if these same macromolecules also contribute to other selectin-mediated cell adhesion processes in humans, like hematopoietic stem cell homing, lymphocyte adhesion and tumor metastasis.

## Supplementary Material

Refer to Web version on PubMed Central for supplementary material.

## Acknowledgments

Sources of funding: Supported by the National Institutes of Health grants HL103411 and HL63014 (to S.N.) and the Biotechnology and Biological Sciences Research Council Grant BB/K016164/1 (to A. D. and S. M. H.).

## References

1. Zarbock A, Ley K, McEver RP, Hidalgo A. Leukocyte ligands for endothelial selectins: specialized glycoconjugates that mediate rolling and signaling under flow. Blood. 2011; 118:6743–6751. [PubMed: 22021370]

2. Vestweber D, Blanks JE. Mechanisms that regulate the function of the selectins and their ligands. Physiol Rev. 1999; 79:181–213. [PubMed: 9922371]

3. Mondal N, Buffone A Jr, Neelamegham S. Distinct glycosyltransferases synthesize E-selectin ligands in human vs. mouse leukocytes. Cell Adh Migr. 2013; 7:288–292. [PubMed: 23590904]

4. Beauharnois ME, Lindquist KC, Marathe D, Vanderslice P, Xia J, Matta KL, Neelamegham S. Affinity and kinetics of sialyl Lewis-X and core-2 based oligosaccharides binding to L- and P-selectin. Biochemistry. 2005; 44:9507–9519. [PubMed: 15996105]

5. Wild MK, Huang MC, Schulze-Horsel U, van der Merwe PA, Vestweber D. Affinity, kinetics, and thermodynamics of E-selectin binding to E-selectin ligand-1. J Biol Chem. 2001; 276:31602–31612. [PubMed: 11404363]

6. Mehta P, Cummings RD, McEver RP. Affinity and kinetic analysis of P-selectin binding to P-selectin glycoprotein ligand-1. J Biol Chem. 1998; 273:32506–32513. [PubMed: 9829984]

7. Buffone A Jr, Mondal N, Gupta R, McHugh KP, Lau JT, Neelamegham S. Silencing alpha1,3-fucosyltransferases in human leukocytes reveals a role for FUT9 enzyme during E-selectin-mediated cell adhesion. J Biol Chem. 2013; 288:1620–1633. [PubMed: 23192350]

8. Xia L, Ramachandran V, McDaniel JM, Nguyen KN, Cummings RD, McEver RP. N-terminal residues in murine P-selectin glycoprotein ligand-1 required for binding to murine P-selectin. Blood. 2003; 101:552–559. [PubMed: 12393631]

9. Sako D, Comess KM, Barone KM, Camphausen RT, Cumming DA, Shaw GD. A sulfated peptide segment at the amino terminus of PSGL-1 is critical for P-selectin binding. Cell. 1995; 83:323–331. [PubMed: 7585949]

10. Wilkins PP, McEver RP, Cummings RD. Structures of the O-glycans on P-selectin glycoprotein ligand-1 from HL-60 cells. J Biol Chem. 1996; 271:18732–18742. [PubMed: 8702529]

11. Lo CY, Antonopoulos A, Gupta R, Qu J, Dell A, Haslam SM, Neelamegham S. Competition between core-2 GlcNAc-transferase and ST6GalNAc-transferase regulates the synthesis of the leukocyte selectin ligand on human P-selectin glycoprotein ligand-1. J Biol Chem. 2013; 288:13974–13987. [PubMed: 23548905]

12. Bochner BS, Sterbinsky SA, Bickel CA, Werfel S, Wein M, Newman W. Differences between Human Eosinophils and Neutrophils in the Function and Expression of Sialic Acid-Containing Counterligands for E-Selectin. J Immunol. 1994; 152:774–782. [PubMed: 7506734]

13. Larsen GR, Sako D, Ahern TJ, Shaffer M, Erban J, Sajer SA, Gibson RM, Wagner DD, Furie BC, Furie B. P-selectin and E-selectin. Distinct but overlapping leukocyte ligand specificities. J Biol Chem. 1992; 267:11104–11110. [PubMed: 1375936]

14. Hidalgo A, Peired AJ, Wild MK, Vestweber D, Frenette PS. Complete identification of E-selectin ligands on neutrophils reveals distinct functions of PSGL-1, ESL-1, and CD44. Immunity. 2007; 26:477–489. [PubMed: 17442598]

15. Levinovitz A, Muhlhoff J, Isenmann S, Vestweber D. Identification of a glycoprotein ligand for E-selectin on mouse myeloid cells. J Cell Biol. 1993; 121:449–459. [PubMed: 7682218]

16. Merzaban JS, Burdick MM, Gadhoum SZ, Dagia NM, Chu JT, Fuhlbrigge RC, Sackstein R. Analysis of glycoprotein E-selectin ligands on human and mouse marrow cells enriched for hematopoietic stem/progenitor cells. Blood. 2011; 118:1774–1783. [PubMed: 21659548]

17. Tiemeyer M, Swiedler SJ, Ishihara M, Moreland M, Schweingruber H, Hirtzer P, Brandley BK. Carbohydrate ligands for endothelial-leukocyte adhesion molecule 1. Proc Natl Acad Sci U S A. 1991; 88:1138–1142. [PubMed: 1705026]

18. Stroud MR, Handa K, Salyan ME, Ito K, Levery SB, Hakomori S, Reinhold BB, Reinhold VN. Monosialogangliosides of human myelogenous leukemia HL60 cells and normal human leukocytes. 2. Characterization of E-selectin binding fractions, and structural requirements for physiological binding to E-selectin. Biochemistry. 1996; 35:770–778. [PubMed: 8547257]

19. Handa K, Stroud MR, Hakomori S. Sialosyl-fucosyl Poly-LacNAc without the sialosyl-Lex epitope as the physiological myeloid cell ligand in E-selectin-dependent adhesion: studies under static and dynamic flow conditions. Biochemistry. 1997; 36:12412–12420. [PubMed: 9376344]

20. Nimrichter L, Burdick MM, Aoki K, Laroy W, Fierro MA, Hudson SA, Von Seggern CE, Cotter RJ, Bochner BS, Tiemeyer M, Konstantopoulos K, Schnaar RL. E-selectin receptors on human leukocytes. Blood. 2008; 112:3744–3752. [PubMed: 18579791]

21. Varki A. Selectin ligands: will the real ones please stand up? J Clin Invest. 1997; 99:158–162. [PubMed: 9005982]
22. Seito N, Yamashita T, Tsukuda Y, Matsui Y, Urita A, Onodera T, Mizutani T, Haga H, Fujitani N, Shinohara Y, Minami A, Iwasaki N. Interruption of glycosphingolipid synthesis enhances osteoarthritis development in mice. Arthritis Rheum. 2012; 64:2579–2588. [PubMed: 22391889]
23. Ichikawa S, Hirabayashi Y. Glucosylceramide synthase and glycosphingolipid synthesis. Trends Cell Biol. 1998; 8:198–202. [PubMed: 9695839]
24. Symington FW, Hedges DL, Hakomori S. Glycolipid antigens of human polymorphonuclear neutrophils and the inducible HL-60 myeloid leukemia line. J Immunol. 1985; 134:2498–2506. [PubMed: 3855933]
25. Mondal N, Buffone A Jr, Stolfa G, Antonopoulos A, Lau JT, Haslam SM, Dell A, Neelamegham S. ST3Gal-4 is the primary sialyltransferase regulating the synthesis of E-, P-, and L-selectin ligands on human myeloid leukocytes. Blood. 2015; 125:687–696. [PubMed: 25498912]
26. Zhang Y, Neelamegham S. Estimating the efficiency of cell capture and arrest in flow chambers: study of neutrophil binding via E-selectin and ICAM-1. Biophys J. 2002; 83:1934–1952. [PubMed: 12324413]
27. Ichikawa, S., Hirabayashi, Y. [33] Genetic approaches for studies of glycolipid synthetic enzymes. In: Alfred, H., Merrill, JYAH., editors. Methods in Enzymology. Vol. 311. Academic Press; 2000. p. 303-318.
28. Cong L, Ran FA, Cox D, Lin S, Barretto R, Habib N, Hsu PD, Wu X, Jiang W, Marraffini LA, Zhang F. Multiplex genome engineering using CRISPR/Cas systems. Science. 2013; 339:819–823. [PubMed: 23287718]
29. Liang JC, Ning Y, Wang RY, Padilla-Nash HM, Schrock E, Soenksen D, Nagarajan L, Ried T. Spectral karyotypic study of the HL-60 cell line: detection of complex rearrangements involving chromosomes 5, 7, and 16 and delineation of critical region of deletion on 5q31.1. Cancer Genet Cytogenet. 1999; 113:105–109. [PubMed: 10484974]
30. Atilla-Gokcumen GE, Bedigian AV, Sasse S, Eggert US. Inhibition of glycosphingolipid biosynthesis induces cytokinesis failure. J Am Chem Soc. 2011; 133:10010–10013. [PubMed: 21668028]
31. Atilla-Gokcumen GE, Muro E, Relat-Goberna J, Sasse S, Bedigian A, Coughlin ML, Garcia-Manyes S, Eggert US. Dividing cells regulate their lipid composition and localization. Cell. 2014; 156:428–439. [PubMed: 24462247]
32. Macher BA, Buehler J, Scudder P, Knapp W, Feizi T. A novel carbohydrate, differentiation antigen on fucogangliosides of human myeloid cells recognized by monoclonal antibody VIM-2. J Biol Chem. 1988; 263:10186–10191. [PubMed: 3164721]
33. Smith CW, Rothlein R, Hughes BJ, Mariscalco MM, Rudloff HE, Schmalstieg FC, Anderson DC. Recognition of an endothelial determinant for CD 18-dependent human neutrophil adherence and transendothelial migration. J Clin Invest. 1988; 82:1746–1756. [PubMed: 2903180]
34. Kunkel EJ, Ley K. Distinct Phenotype of E-Selectin Deficient Mice: E-Selectin Is Required for Slow Leukocyte Rolling In Vivo. Circulation Research. 1996; 79:1196–1204. [PubMed: 8943958]
35. Puri KD, Finger EB, Springer TA. The faster kinetics of L-selectin than of E-selectin and P-selectin rolling at comparable binding strength. J Immunol. 1997; 158:405–413. [PubMed: 8977216]
36. Liu Z, Miner JJ, Yago T, Yao L, Lupu F, Xia L, McEver RP. Differential regulation of human and murine P-selectin expression and function in vivo. J Exp Med. 2010; 207:2975–2987. [PubMed: 21149548]
37. Moore KL, Patel KD, Bruehl RE, Li F, Johnson DA, Lichenstein HS, Cummings RD, Bainton DF, McEver RP. P-selectin glycoprotein ligand-1 mediates rolling of human neutrophils on P-selectin. J Cell Biol. 1995; 128:661–671. [PubMed: 7532174]
38. Ohmori K, Fukui F, Kiso M, Imai T, Yoshie O, Hasegawa H, Matsushima K, Kannagi R. Identification of cutaneous lymphocyte-associated antigen as sialyl 6-sulfo Lewis X, a selectin ligand expressed on a subset of skin-homing helper memory T cells. Blood. 2006; 107:3197–3204. [PubMed: 16380447]

39. Picker LJ, Michie SA, Rott LS, Butcher EC. A unique phenotype of skin-associated lymphocytes in humans. Preferential expression of the HECA-452 epitope by benign and malignant T cells at cutaneous sites. Am J Pathol. 1990; 136:1053–1068. [PubMed: 1693467]

40. Wagers AJ, Stoolman LM, Kannagi R, Craig R, Kansas GS. Expression of leukocyte fucosyltransferases regulates binding to E-selectin: relationship to previously implicated carbohydrate epitopes. J Immunol. 1997; 159:1917–1929. [PubMed: 9257857]

41. Fukushima K, Hirota M, Terasaki PI, Wakisaka A, Togashi H, Chia D, Suyama N, Fukushi Y, Nudelman E, Hakomori S. Characterization of sialosylated Lewisx as a new tumor-associated antigen. Cancer Res. 1984; 44:5279–5285. [PubMed: 6386148]

42. Liu G, Neelamegham S. Integration of systems glycobiology with bioinformatics toolboxes, glycoinformatics resources, and glycoproteomics data. Wiley Interdiscip Rev Syst Biol Med. 2015; 7:163–181. [PubMed: 25871730]

## Abbreviations

| | |
|---|---|
| **UGCG** | UDP-Glucose Ceramide Glucosyltransferase |
| **GSL** | Glycosphingolipids or Glycolipids |
| **PSGL-1** | P-selectin glycoprotein ligand-1 |
| **sLe$^X$** | sialyl Lewis-X |

## SIGNIFICANCE

The binding of specific glycoconjugates expressed on human myeloid cell surfaces to E-selectin on endothelial cells controls the progress of a variety of human inflammatory diseases. The identification of such glycans on human leukocytes is important since inhibitors that block their binding to E-selectin can result in novel anti-inflammatory therapies. Using genetic approaches (lentiviral shRNA and CRISPR-Cas9 knockouts), the current manuscript unambiguously demonstrates that sialofucosylated glycosphingolipids (GSLs) expressed on the surface of human, but not murine, myeloid cells can bind E-selectin under physiological fluid shear conditions. Such GSL binding to E-selectin likely controls the rate at which human leukocytes of the myeloid lineage transition from rolling interactions on the vessel wall to firm arrest at sites of inflammation. Blocking GSL biosynthesis results in leukocytes exhibiting skipping or unstable rolling interactions, and reduced diapedesis across the endothelium.

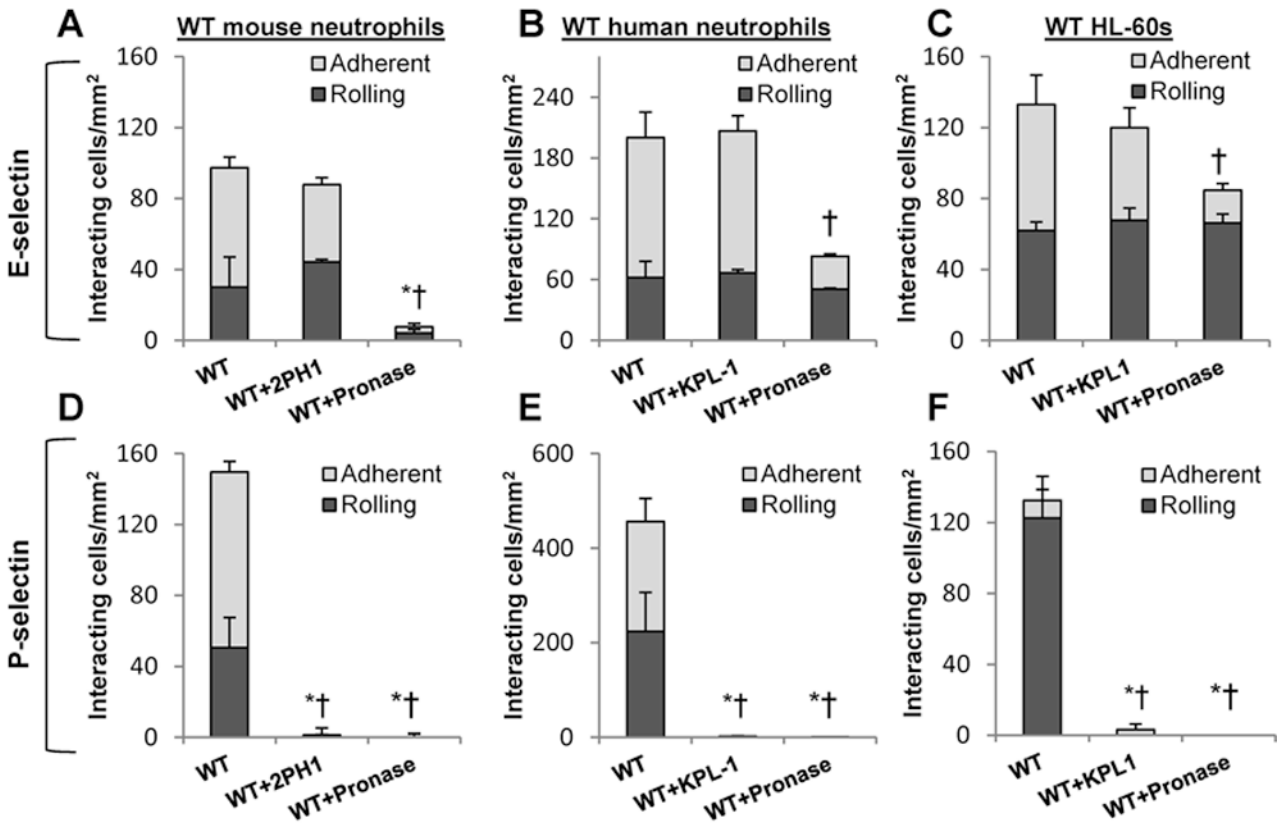


**Figure 1. Rolling of human and mouse neutrophils on E- and P-selectin**

$2\times10^6$/mL WT mouse neutrophils (panel A, D), human neutrophils (B, E) or HL-60 cells (C, F) were perfused over substrates bearing either E- (top panels), or P-selectin (bottom panels) at 1 dyne/cm$^2$. Substrates were composed of either E-selectin expressing IL-1β stimulated HUVECs (A-C) or physisorbed recombinant P-selectin (D-F). In some cases, the cells were treated with 1mg/mL pronase for 1h at 37°C prior to perfusion. Individual bars in each panel present the rolling (dark) and adherent (light) cell density 2 min after the start of perfusion. 2PH1 and KPL-1 are blocking mAbs against murine and human PSGL-1, respectively. * and † represent statistically significant differences for rolling and adherent cells, respectively ($P$<0.05 with respect to all other treatments except *s and †s are not different from each other).

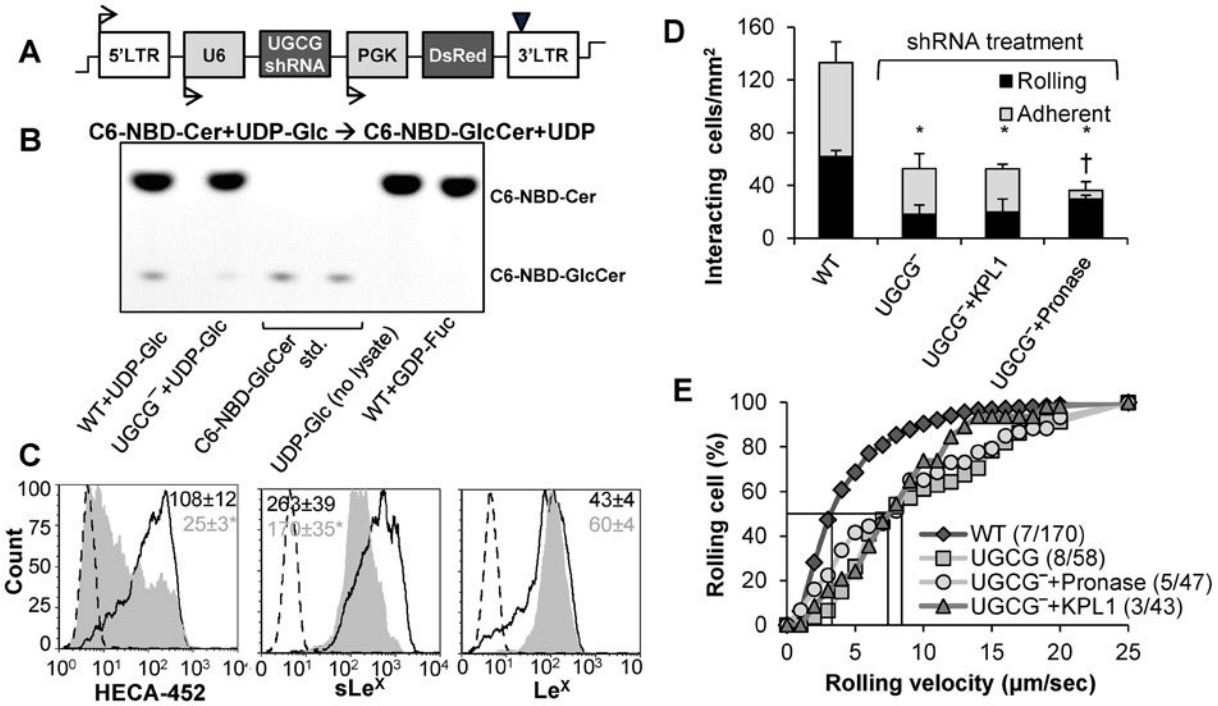


**Figure 2. Silencing UGCG in HL-60s**

**A.** pLKO.1 lentiviral vector with DsRed reporter and UGCG shRNA was used to create stable UGCG⁻HL-60 cells. **B.** TLC of UGCG enzyme assay shows activity reduction in the UGCG⁻HL-60 cell lysate (lane 2) compared to WT HL-60 (lane 1). C6-NBD-GlcCer product standards serve as positive control (lanes 3, 4). Negative controls either lack cell lysate (lane 5) or contain GDP-Fuc in place of UDP-Glc (lane 6). **C.** Flow cytometry histograms showing cell-surface expression of CLA/HECA-452 (left), sialyl Lewis-X/CD15s/CSLEX-1 (middle) and Lewis-X/CD15 (right). Black-empty and shaded histograms correspond to WT and UGCG⁻HL-60s. Dashed-empty histograms correspond to isotype controls. Silencing UGCG reduced cell-surface CLA and $sLe^X$ expression. **D-E.** Rolling and adherent cell density (D) and cumulative rolling velocity distribution (E) data for WT and UGCG⁻HL-60s perfused over IL-1β stimulated HUVECs at 1 dyn/cm$^2$. Statistical symbols are same as Fig. 1. Cells with reduced UGCG activity displayed ~60% reduced rolling and adherent cell density and ~2 fold higher rolling velocity. Pronase further reduced the number of adherent UGCG⁻HL-60s. Numbers in brackets present '(number of experiments/total number of cells analyzed)'.

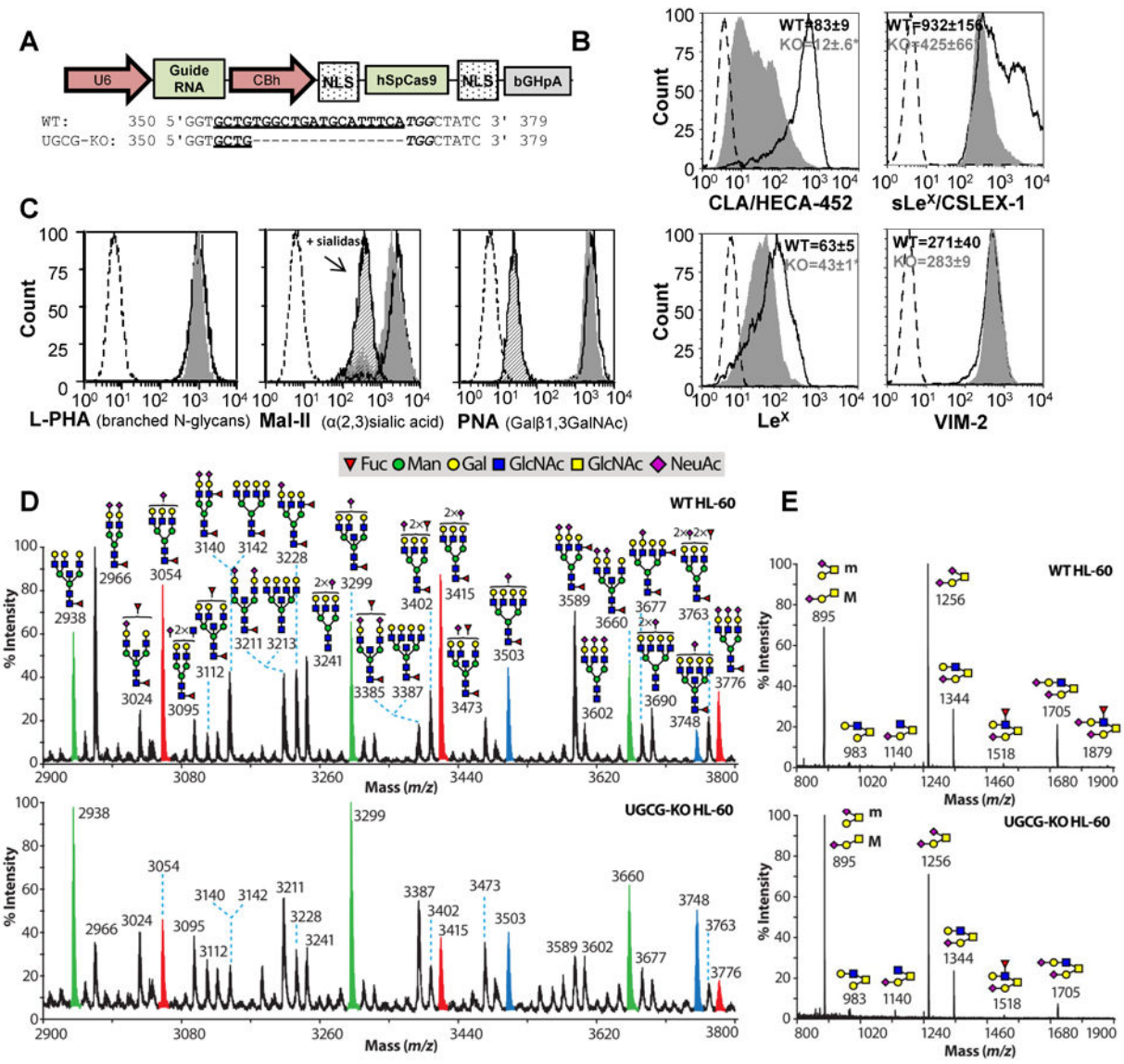


**Figure 3. UGCG knockout HL-60s**

**A.** Schematic of CRISPR-Cas9 editing vector used to create knockout HL-60 cells lacking UGCG. Top row presents WT HL-60 UGCG sequence while bottom row shows 16bp chromosomal deletion in the UGCG-KO cells. Bold-underlined text highlights the guide RNA sequence and the bold-italicized text denotes the protospacer adjacent motif (PAM/NGG). Only one UGCG allele was sequenced since UGCG is present on chromosome-9, and spectral karyotyping of HL-60 demonstrates the loss of the second copy due to the chromosome-9 translocation. **B.** Flow cytometry histograms present cell surface expression of CLA/HECA-452, sLe$^X$/CSLEX-1, Le$^X$/CD15 and VIM-2/CD65s epitopes on WT (black-empty histogram) and UGCG-KO HL-60s (gray-filled). Dashed-empty histogram is isotype control. Mean ± SEM data for WT and KO cells is presented in inset. **C.** L-PHA-FITC (left), Mal-II-biotin (middle) and PNA-FITC (left) lectin binding to WT (black-empty) and UGCG-KO (gray-filled) HL-60s measured using flow cytometry. Prior to PNA-FITC

staining, the cells were desialylated using α2,3/6/8/9 neuraminidase from *A. ureafaciens*. In all panels, dashed (- -) histograms correspond to cells alone without lectins. Cells incubated with Mal-II-biotin were subsequently detected using α-biotin-FITC. Hatched peaks indicate negative controls: WT cells treated with neuraminidase (middle) and without neuraminidase (right). UGCG knockouts display reduction in CLA and $sLe^X$ epitopes (*$P$<0.05 with respect to WT), but no major change in lectin binding. **D.** Partial MALDI-TOF MS spectra of permethylated N-glycans of WT (upper panel) and UGCG-KO (lower panel) HL-60 cells. Spectra are from the 50% acetonitrile fraction. Red peaks correspond to decreased sialylated structures, while green peaks correspond to increased bisected structures, in the UGCG-KO HL-60s (lower panel). The increase in bisected N-glycans in the UGCG-KO is supported by comparing the relative intensity of ions at *m/z* 3748 to 3503 (blue peaks). In WT, the ratio of these peaks is 0.356. In the UGCG-KO it is 1.183, thus suggesting a ~232% increase in bisected structures in the UGCG-KO HL-60s. Full spectra are shown in Supplemental Fig. IV. **E.** MALDI-TOF MS spectra of permethylated O-glycans of WT (top) and UGCG-KO (bottom) HL-60 cells. Spectra are from the 35% acetonitrile fraction. Annotated structures are according to the Consortium for Functional Glycomics guidelines. All molecular ions are $[M+Na]^+$. Putative structures are based on composition, tandem MS/MS (data not shown), and biosynthetic knowledge. Cartoons that include sugar symbols outside a bracket have not been unequivocally defined. Letters “m” and “M” in bold characters indicate minor and major abundances respectively.

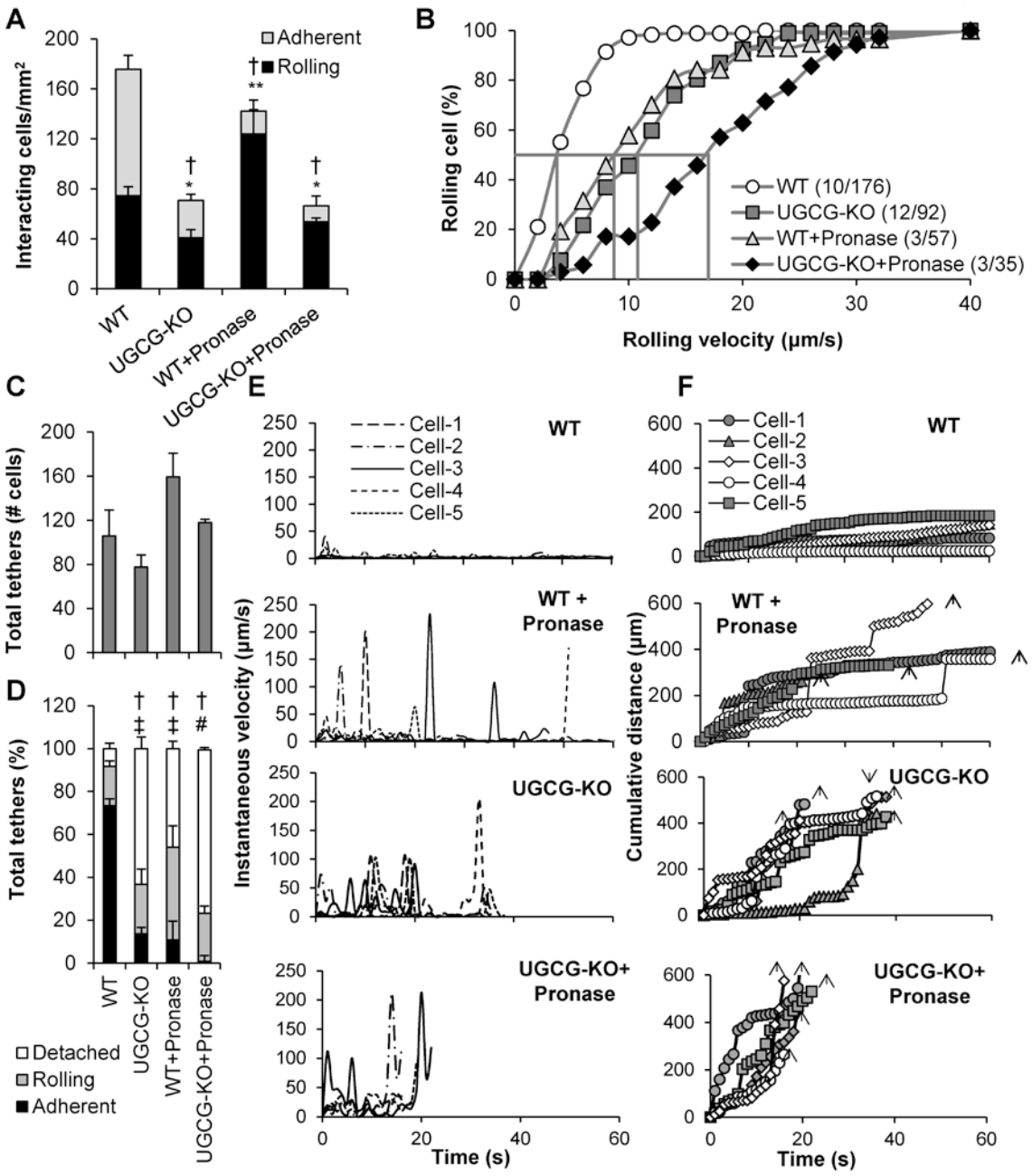


**Figure 4. E-selectin mediated rolling of UGCG-KO HL-60s**

**A-B.** Rolling and adherent cell density (panel A) and rolling velocity distribution (B) data for UGCG-KO HL-60s measured under conditions in Fig. 2D and 2E, respectively. Statistical symbols are same as Fig. 1. In addition, ** denotes statistically significant difference ($P$<0.05) in cell rolling with respect to all other treatments. UGCG-KO HL-60s display ~60% reduced rolling and adherent cell density, with ~3 fold higher median rolling velocity compared to WT HL60s. Pronase further increased rolling velocity. **C.** Individual columns present total number of cell tethers formed in a 4 min interval. Number of tethers did not vary significantly with cell type or upon pronase treatment. **D.** Tethered cells

(normalized to 100%) were classified into: i. adherent, ii. rolling or iii. detached cells as defined in Methods.Cell detachment was prominent in UGCG-KO HL-60 cells (For detached cells: ‡$P$<0.05 with respect to all treatments except ‡s are not different from each other, and #$P$<0.05 with respect to all other treatments). Number of adherent cells is also highest for WT HL60s (†$P$<0.05 with respect to all treatments except †s are not different from each other). **E.** Instantaneous rolling velocity and F. cumulative distance travelled with time for five representative cells for each treatment. WT HL-60s rolled stably at 3-15 μm/s, whereas all the other cell types show abrupt increases in rolling velocities as seen in the intermittent peaks up to 250μm/s. Detachment events are depicted by up arrows in panel f.

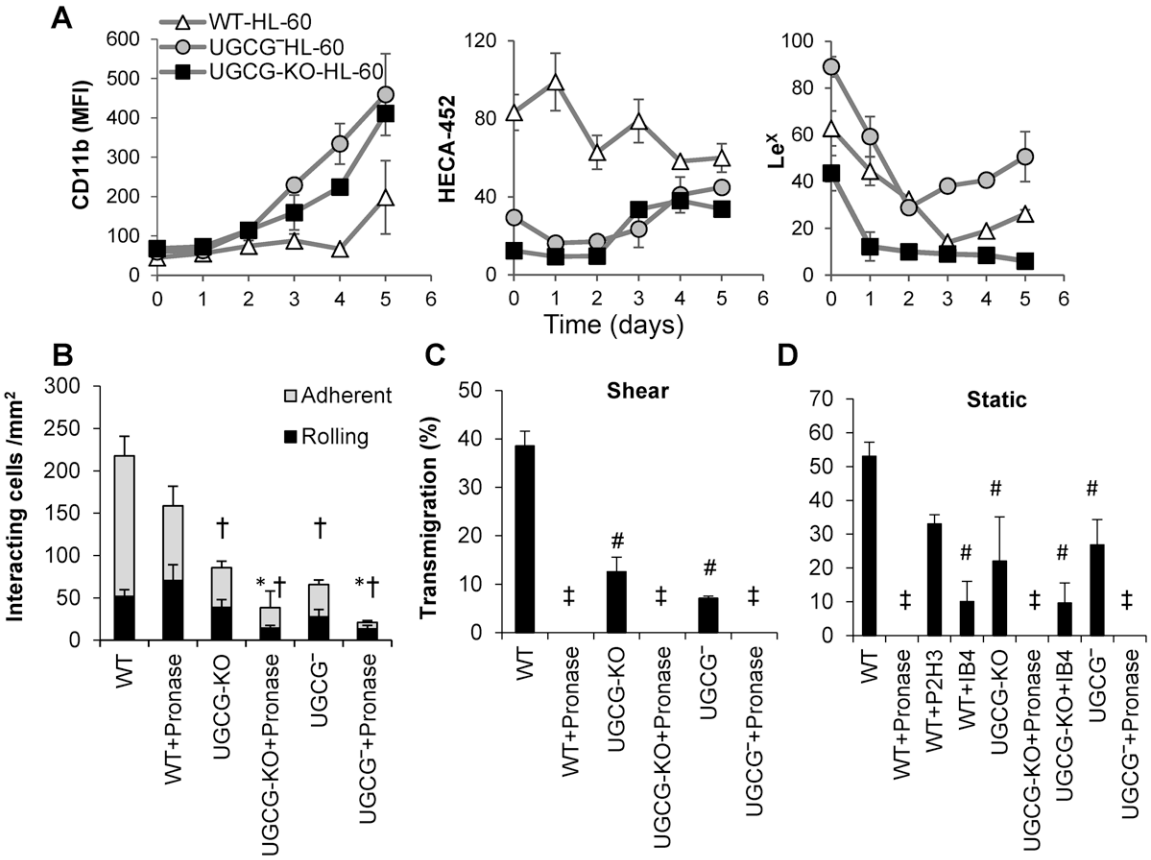


**Figure 5. Studies with differentiated HL-60 cells**

HL-60s were differentiated towards granulocytes by culturing cells in growth medium containing 1.3% DMSO for 5 days. **A.** Cell surface glycan and glycoprotein expression over the course of differentiation. **B.** Rolling and adherent cell density data for differentiated cells binding to stimulated HUVEC monolayers at 1dyn/cm$^2$ with or without pronase treatment. Experimental method and statistical symbols are identical to Fig. 1. **C.-D.** % Transmigration, under shear (C) and static (no flow, D) conditions. Plot quantifies the % of total interacting cells in a FOV that transmigrated during a 20 min interval. ‡ and # denote $P$<0.05 with respect to all treatments, except these symbols are not different from each other. Increased cell detachment of UGCG-KO and UGCG⁻HL-60s reduced transmigration under shear.

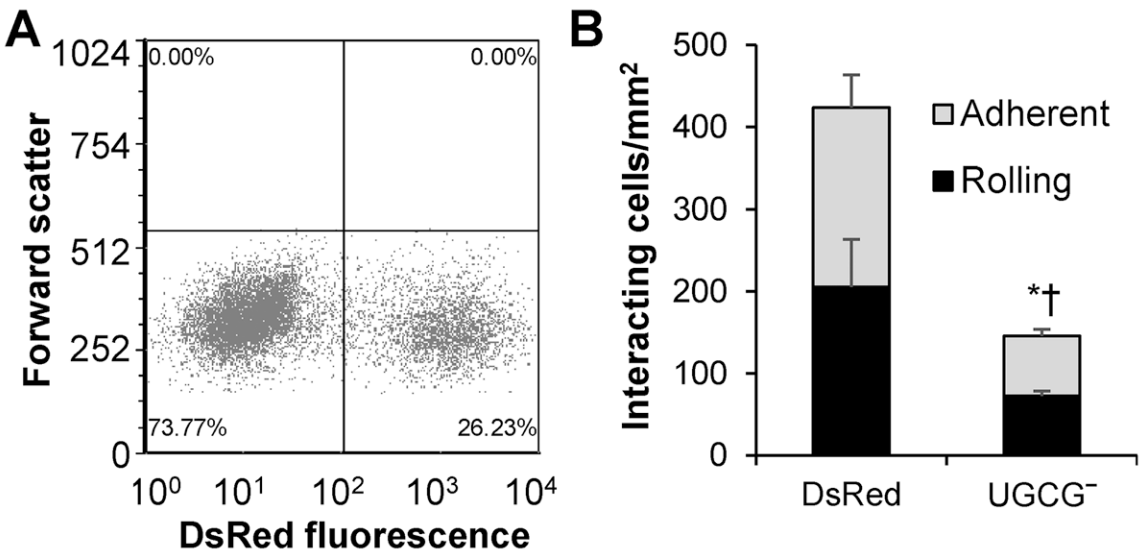


**Figure 6. Neutrophils derived from human hematopoietic stem cells (hHSCs)**

hHSCs were differentiated to mature neutrophils over 12 days. 'UGCG$^{-}$-Neu' were generated using lentivirus carrying a DsRed reporter and UGCG shRNA. Control cells generated using a vector lacking the shRNA was called 'DsRed-Neu'. **A.** Transduction efficiency quantified based on % cells that were DsRed positive (bottom-right quadrant). **B.** Rolling and adherent cell density data for DsRed$^{+}$ neutrophils derived from hHSCs on IL-1β stimulated HUVECs. * and † denote statistically lower rolling and adherent cell density on E-selectin upon silencing UGCG ($P$<0.05 with respect to WT). Data are presented for hHSCs derived from 4 different human donors.